

Andrea Brækken & Jenny Bakken

Does exercised plasma have an effect on amyloid-beta and microglia in an Alzheimer's Disease rat model?

Bacheloroppgave i Bioingeniørfag

Veileder: Aleksi M. Huuha, Ragnhild E. N. Røsbjørgen, Nathan Scrimgeour, Atefe R. Tari & Kaisa Lehti

Mai 2022

Andrea Brækken & Jenny Bakken

Does exercised plasma have an effect on amyloid-beta and microglia in an Alzheimer's Disease rat model?

Bacheloroppgave i Bioingeniørfag

Veileder: Aleksi M. Huuha, Ragnhild E. N. Røsbjørgen, Nathan Scrimgeour, Atefe R. Tari & Kaisa Lehti

Mai 2022

Norges teknisk-naturvitenskapelige universitet

Fakultet for naturvitenskap

Institutt for bioingeniørfag



Kunnskap for en bedre verden

Acknowledgments

This bachelor's thesis was carried out at the Cardiac Exercise Research Group (CERG), at the Department of Circulation and Medical Imaging, Faculty of Medicine and Health Sciences at The Norwegian University of Science and Technology in Trondheim. This assignment was a part of the subject "Bacheloroppgave i Bioingeniørfag", course code HBIO3001, Faculty of Natural Sciences at The Norwegian University of Science and Technology, and completes the bachelor's degree in Bioingeniørfag.

First and foremost, we would like to thank CERG for giving us the opportunity to do the project work at your facilities. It has been very educational and inspiring to be a part of your research environment. Writing this paper has been interesting and challenging, and our learning curve has been steep. We have learned a lot about the health effects of exercise, the global health issue that Alzheimer's disease is, but also a lot about the process and execution of medical research.

We would also want to take this opportunity to thank our amazing bachelor supervisors; Aleksi Matias Huuha, Ragnhild E. N. Røsbjørgen, Nathan Scrimgeour, Atefe R. Tari and Kaisa Lehti for their helpful guidance and constructive feedback. A special thanks to Aleksi Matias Huuha for your patience, help with laboratory experiments, writing process, and follow-up throughout the process no matter what time or regard.

In the end, we would also like to thank each other for amazing teamwork, for helping each other out when needed, and for every fun moment, we have had together.

Trondheim, May 20th, 2022

Andrea Brækken

Andrea Brækken

Jenny Bakken
Jenny Bakken

Abstract

The risk of developing Alzheimer's disease (AD) increases with aging, and due to increased life expectancy among humans, a larger proportion of the world's population will be affected by the disease in the future. This will lead to a burden for healthcare systems and carers and a great financial cost for the world community. The need for medicine that prevents the development or treats the disease is increasing, and there is currently no available cure in this field.

Exercise has been associated with reduced AD risk, which might be partly due to exercise-induced changes in the blood. One of the earliest hallmarks of AD is the formation of amyloid-beta ($A\beta$) plaques in the subiculum region in the brain. The reduction of $A\beta$ accumulation would reduce the formation of $A\beta$ plaques, which would be reflected in less activation of microglial cells in the brain. The microglial cells are phagocytic cells that survey the brain for $A\beta$ or debris. When phagocytosing they become active, characterized by few and short branches.

To investigate if plasma from exercised donors could have a beneficial effect on $A\beta$ accumulation and microglial activation state, rats from three different groups were compared; untreated wild-type rats, untreated AD rats, and exercised plasma-treated AD rats (ExPlas rats). The rat brain tissue was stained using an immunofluorescence staining protocol, imaged using confocal microscopy, and analyzed for quantity of $A\beta$ and morphology of microglial cells.

The results show a significant difference when it came to the increased number of microglial cells in the ExPlas brains compared to the brains of the wild-type rats ($p=0.008$). There were longer branches per microglial cell in the wild-type rats and the ExPlas rats, compared to the brains of the AD rats ($p=0.031$, $p=0.040$, respectively), which indicates less active cells. In the ExPlas brains there were more endpoints per microglial cell compared to the brains of the AD rats ($p=0.040$). Due to the high level of what is presumed to be autofluorescence, the planned analyses of $A\beta$ were not feasible.

We found that there were more similarities between the microglial cells in the wild-type rats and ExPlas rats, compared to the AD rats. This most likely indicates that exercised plasma treatment on rats expressing AD pathology has a beneficial effect on the microglial state.

Sammendrag

Risikoen for å utvikle Alzheimers sykdom (AD) øker med alderen, og på grunn av at forventet levealder øker, vil en større del av verdens befolkning bli berørt av sykdommen i fremtiden. Dette vil medføre en større belastning for helsevesen og omsorgspersoner, og en økt kostnad for verdenssamfunnet. Det er for øyeblikket ingen tilgjengelig kur som enten kan forhindre utviklingen eller behandle sykdommen, selv om behovet er økende.

Trening har blitt assosiert med redusert AD-risiko, noe som kan skyldes treningsinduserte forandringer i blodet. Plakkdannelse av amyloid-beta ($A\beta$) i subiculum-området i hjernen er et av de tidligste kjennetegnene på AD. Reduksjon av $A\beta$ -dannelse i hjernen kan resultere i mindre plakkdannelse, som igjen vil kunne føre til mindre aktivisering av mikroglia-celler i hjernen. Mikroglia-celler er fagocytterende celler som overvåker hjernen for $A\beta$, og annet avfall. Ved fagocyttering blir cellene aktive, som kjennetegnes med få og korte cellegrener.

For å undersøke om trent plasma kan ha gunstig effekt på $A\beta$ -dannelsen, og aktiveringen av mikroglia-celler, ble rotter fra tre ulike grupper sammenlignet; ubehandlede vill-type-rotter, ubehandlede AD-rotter og AD-rotter som ble behandlet med trent plasma (ExPlas-rotter). Hjernevev fra rottene ble farget ved hjelp av en immunfluorescensprotokoll, og avbildet ved bruk av konfokalmikroskopi for å analysere mengde $A\beta$ og morfologien til mikroglia-cellene.

Resultatet viste en signifikant forskjell når det kom til det økte antallet mikroglia-celler i ExPlas-rottene hjerne, sammenlignet med vill-type-rottene ($p=0.008$). Det var lengre cellegrener per mikroglia-celle i vill-type-rottene og ExPlas-rottene, sammenlignet med hjernene til AD-rottene (henholdsvis $p=0.031$, $p=0,040$), noe som indikerer mindre aktive celler. I ExPlas-hjernene var det flere endepunkter per mikroglia-celle, sammenlignet med hjernene til AD-rottene ($p=0.040$). På grunn av høye nivåer av det som antas å være autofluorescens, var det ikke mulig å gjennomføre de planlagte analysene på $A\beta$.

Vi fant ut at det var flere likheter mellom mikroglia-cellene i vill-type-rottene og ExPlas-rottene, sammenlignet med AD-rottene. Mest sannsynlig indikerer dette at behandling med trent plasma på rotter med AD-patologi har en gunstig effekt på mikroglia-cellenes tilstand.

Contents

Acknowledgments.....	I
Abstract.....	II
Sammendrag	III
Abbreviations.....	VI
1.0 Introduction.....	1
1.1 Alzheimer’s disease	2
1.1.1 Stages of Alzheimer’s disease.....	2
1.1.2 What is amyloid-beta?	3
1.1.3 Areas in the brain that are affected by Alzheimer’s disease	3
1.2 Neuroinflammation	4
1.2.1 The glial cells astrocytes and microglia.....	5
1.2.2 Microglial cells and Alzheimer’s disease	5
1.3 Physical activity and Alzheimer’s disease.....	6
1.4 Could circulation molecules mediate effects of exercise to the brain?	7
1.4.1 Studies with mice.....	7
1.4.2 Transgenic rat models of Alzheimer’s disease.....	8
1.5 The ExPlas study.....	9
1.6 Immunohistochemistry	10
1.6.1 Antigen-antibody interactions.....	10
1.6.2 Heat-induced antigen retrieval	11
1.7 Immunofluorescence.....	12
1.7.1 Fluorescence microscopy.....	13
1.7.2 Confocal microscope.....	14
1.8 Aim of this project	15
2.0 Materials and methods	16

2.1 Project design.....	16
2.2 Rat models	17
2.3 Immunofluorescence staining protocol for amyloid-beta and microglia	17
2.3.1 Positive and negative controls.....	18
2.3.2 Changes and modifications of the protocol.....	18
2.4 Detection and quantification	19
2.4.1 Image acquisition and skeleton analysis	19
2.4.2 Statistical analyses	20
3.0 Results.....	21
3.1 Amyloid-beta and microglial cells combined	21
3.2 Microglial cells	22
3.3 Amyloid-beta	28
3.4 Controls.....	29
4.0 Discussion.....	30
4.1 Microglial cells	30
4.2 Amyloid-beta	32
4.3 Strengths and limitations.....	34
5.0 Conclusion	35
6.0 References.....	36
7.0 Appendix.....	39
Appendix I: Overview of the preclinical ExPlas study	39
Appendix II: Overview of the rat models	41
Appendix III: Staining protocol for detecting amyloid-beta and microglial cells	42
Appendix IV: Solutions preparing for the immunostaining protocol	43

Abbreviations

A β	Amyloid-beta
Ab	Antibody
Abs	Antibodies
AD	Alzheimer's disease
Ag	Antigen
Ags	Antigens
APP	Amyloid precursor protein
DMSO	Dimethyl Sulfoxide solution
IHC	Immunohistochemistry
MCI	Mild Cognitive Impairment
PA	Physical Activity
PFA	Paraformaldehyde
TBS	Tris-buffered saline
TBS-Tx	Tris-buffered saline Triton X-100

1.0 Introduction

A wide range of disease states in the brain that lead to memory loss and cognitive decline in mammals are referred to as dementia (1). The difference between Alzheimer's disease (AD) and dementia can be challenging to understand. AD is a type of neurodegenerative disease, whereas dementia refers to the symptoms that one gets with this type of brain disease, such as memory loss, difficulties with speaking, problem-solving, and other everyday tasks, such as bathing and cooking (2). AD leads to dementia, and is just one of many causes of dementia, making up about 50 – 70% of all cases (1,2).

The various risk factors for developing AD include genetic variation, diabetes, hypertension, obesity, and cardiovascular diseases (3). The greatest risk factor for AD is old age and due to increased life expectancy, more people will be affected by the disease in the future (4). The worldwide prevalence of dementia is currently (per September 2021) more than 55 million, with approximately 10 million new diagnosed cases every year (5). Over 150 million people are estimated to be living with dementia in 2050, and over 100 million of these with AD (6).

Patients with AD gradually become in need of more care, and in combination with more people affected by age-related impairments, family and social care expenses will be a great financial burden to the world community (1). No available cure exists to prevent or treat AD, although the need is increasing. Therefore, research and development of new treatments to prevent or reverse AD are important.

1.1 Alzheimer's disease

A German neuropathologist called Alois Alzheimer first described AD in 1907, calling it “Dementia Praecox”. This disease can be either genetic (hereditary) or it can appear sporadically (7). Approximately 70% of the risk of developing AD can be linked to genetics (3). AD is a progressive disease, meaning it develops over time and the symptoms slowly become worse. The development of AD is thought to begin approximately 20 years before the first symptoms start to appear (2). The main pathological changes in the brain associated with AD are amyloid-beta ($A\beta$) accumulation and tau-tangles, as well as degeneration of nerve cells (8).

1.1.1 Stages of Alzheimer's disease

The timeline of AD development can be divided into a preclinical stage, Mild Cognitive Impairment (MCI) due to AD, and a stage where the patient has dementia due to AD (Figure 1) (2). Dementia stage can be further divided into three stages based on the severity of the symptoms.

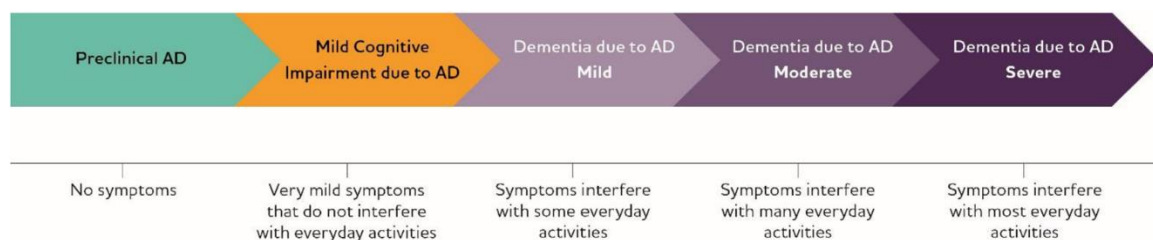


Figure 1. The stages of the development of AD, illustration adapted from The Alzheimer's Association 2022 (8).

Patients in the stage of preclinical AD, do not have symptoms of AD yet, but they may have measurable changes in the brain such as abnormal $A\beta$ (8). MCI due to AD is the first phase where the patients may start to get symptoms like memory problems and problems with thinking and speaking. These symptoms can be difficult to notice if you don't know the person, but close family and friends may perceive the behavior change. A person with MCI can probably live their life normally in the beginning. After two years of MCI, about 15% of the affected people start to develop dementia, and within five years around 30% develop dementia due to AD (2).

Dementia due to AD can be divided into three stages: mild, moderate, and severe AD. In the mild stage, people can function independently with the most basic everyday activities, they just need more time. They may need help with some tasks, such as handling money and paying bills. In the next stage of dementia due to AD, the moderate stage, people will experience more problems with memory and language, and it is harder to perform basic everyday activities, such as bathing and getting dressed. Their personality may change, they can start to behave differently, and for instance, forget their families and friends. When it comes to the last stage of AD, the severe stage disease, the affected people become more in need of care at all hours of the day. Verbal communication becomes hard, and they may not recognize the people around them anymore (8).

1.1.2 What is amyloid-beta?

Amyloid precursor protein (APP) is a protein highly expressed in neurons. The physiological functions of APP are not fully understood, but seem to be related to synaptic functions and cellular development (9). APP can be cleaved to generate A β peptides of different lengths, depending on the type of cleaving proteolytic enzymes. When cleaved by beta- and gamma-secretases, A β peptides with 40 – 42 amino acids are produced. These A β peptides can easily bind together to form A β dimers, which again can form A β oligomers and further polymers that will eventually assemble into the insoluble A β plaques. A β oligomers are thought to be most toxic to neurons (10).

1.1.3 Areas in the brain that are affected by Alzheimer's disease

The hippocampus is an area in the brain that has a major role in learning and the formation of memories (8,11). This area is affected by several neuropsychiatric disorders such as AD. The hippocampus has two parts: the Cornu Ammonis (hippocampus proper) and dentate gyrus. The dentate gyrus has shown to be an area where cognitive decline happens early in both rodents and humans (12). The two parts are separated by the hippocampal sulcus, and under the sulcus is the subiculum (Figure 2) (11). The subiculum is one of the earliest brain regions affected by A β plaque pathology and loss of neurons, both early markers of AD. Therefore it is important to study this region for the detection of A β (13,14).

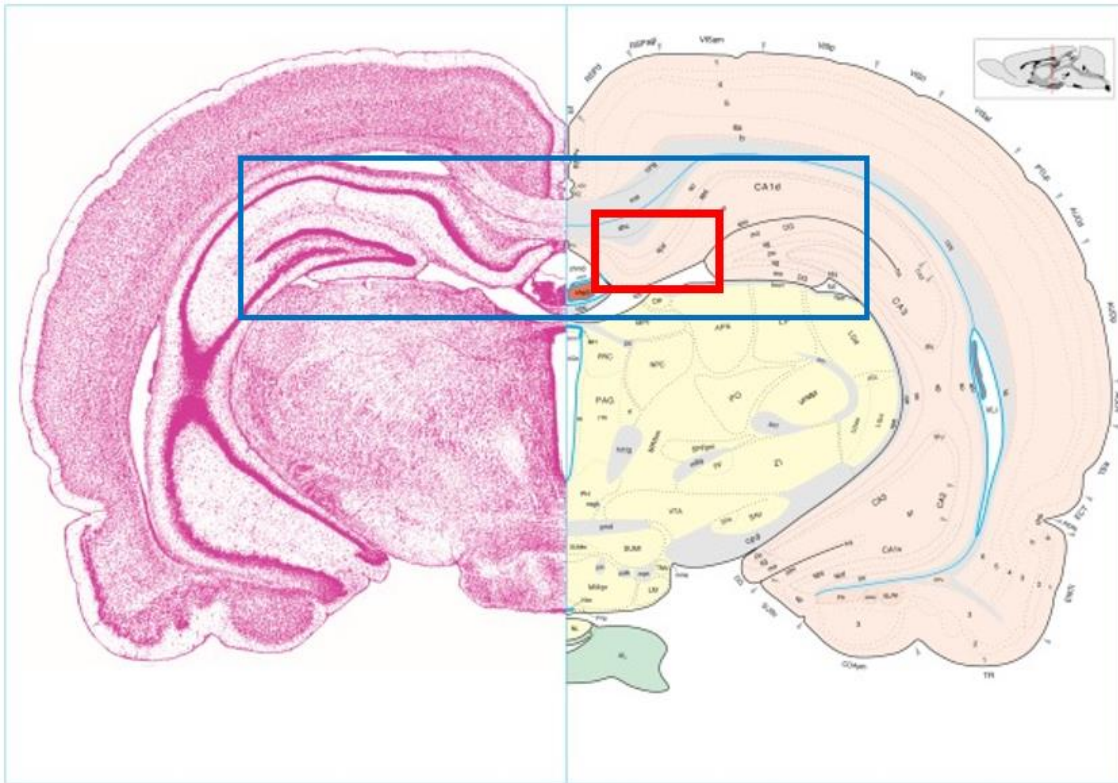


Figure 2. Coronal section of the rat brain; a stained tissue is shown on the left, with a drawing (map) of corresponding regions on the right, including a highlight of the subiculum (red box) and hippocampus (blue box). Illustration adapted and modified from Swanson, Larry W (15).

1.2 Neuroinflammation

Neuroinflammation is inflammation of the central nervous system that can occur as a consequence of aging and different pathological insults, such as infection, trauma, and toxins (16). It is described as an immune response of the brain, where different proinflammatory cytokines and chemokines are produced and released in the brain. This activates microglia and astrocytes, in addition to capillary endothelial cells and infiltrating blood cells. Secretion of proinflammatory molecules can also cause harm to the neurons. It can lead to synaptic dysfunction, neuronal death, and inhibition of neurogenesis (10). Anti-inflammatory cytokines are likewise released during the inflammatory process, to prevent excessive neuroinflammation. If the neuroinflammation fails to resolve by itself, it may develop into a chronic process, ultimately leading to AD. Neuroinflammation therefore has an important role in the pathogenesis of AD (10).

1.2.1 The glial cells astrocytes and microglia

Two types of glial cells in the brain, astrocytes and microglial cells, are involved in AD pathological changes. The astrocytes are specialized glial cells that support the functions of the central nervous system. Astrocytes are important for the metabolism of neurons and provide metabolic support to the synapses that they surround. They also participate in cerebral blood flow circulation and help to eliminate neurotoxic waste, including A β . Together with microglial cells, astrocytes mediate some of the toxic effects of microglia in disease states (10).

The microglial cells are phagocytic immune cells inside the central nervous system, they function throughout the development, maturation, and senescence of the brain. They function in maintaining the health of the brain by removing damaged neurons, and also have an important role in developmental synaptic pruning, as well as in the maintenance of synaptic plasticity and immune surveillance (10).

1.2.2 Microglial cells and Alzheimer's disease

In early stages of AD, microglial cells may phagocytose A β to remove it. These cells can also be found concentrated around A β plaques. The microglial cells migrate to the area where the A β plaques are found and form a microglial cluster around the plaque, potentially getting rid of the A β and other debris. However, abundant evidence exists to suggest that activated microglial cells can also cause harm to the neurons (17).

A microglial cell (Figure 3) contains a cell body (soma) and branches. The number of branches and their endpoints indicates the activation state of the cell. Activated microglial cells that secrete chemokines and cytokines have less branches and endpoints than inactive (surveying) cells (Figures 3A and 3B). When actively phagocytosing, these cells have even fewer branches (16).

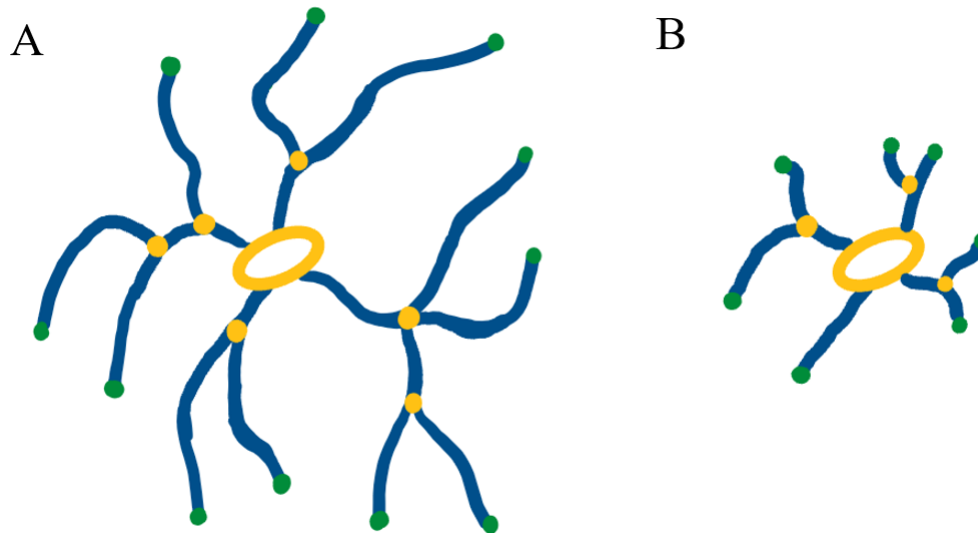


Figure 3. Illustration of microglial cells. A: an inactive microglial cell with many and long branches. B: an active microglial cell with less and shorter branches. Endpoints are displayed in green, branches in blue, and junctions in yellow. Illustration by Jenny Bakken.

1.3 Physical activity and Alzheimer's disease

Many new studies suggest that brain health is closely linked to the overall health of the cardiovascular system and that physical activity (PA) and high cardiorespiratory fitness have a lot of benefits to the body and brain. Several cardiovascular risk factors are also risk factors for AD, and the beneficial effects of exercise training on the brain may be at least partly related to improved cardiovascular health and increased cardiorespiratory fitness. PA is known to be good for the cardiovascular system and reduces the risk of cardiovascular disease and related mortality. Similarly, PA is associated with attenuated cognitive impairment and reduced risk of AD (18).

Importantly, PA may act as a prophylactic and a disease-slowng treatment for dementia. People engaging in high levels of aerobic PA have a lower plasma and brain A β load, which are both strong AD biomarkers (1). All levels of PA have been shown to protect against cognitive decline, and the higher the level of PA, the better the protection. PA also preserves brain volume, including the hippocampal volume, in both animals and humans, which is associated with better cognitive functions (1). These benefits have been linked to systemic neurotrophic factors induced by exercise. Exercise also enhances cerebral blood flow, which

can promote the delivery of neurotrophic factors to the brain (1,19). To study the effects of PA, rat models are often used.

1.4 Could circulation molecules mediate effects of exercise to the brain?

It is not feasible to study pathological changes in human brains, and therefore the use of rodent models is a good alternative for studying the brain and AD. In animal models, the effects of exposure to young blood have been studied on the brain of aged mice and rats on molecular, structural, functional, and cognitive levels. In the last 20 years, transgenic rodent models have been used in research of many diseases, including AD.

1.4.1 Studies with mice

A study by Villeda *et al* showed that cognitive alterations observed in aged mice have been found to be partly reversible following exposure to blood from young mice (4). They discovered that exposure to young blood through heterochronic parabiosis (joined circulations in aged-young pairs) improves cell function in the brain. Exposure to young blood enhanced hippocampal synaptic plasticity and spine number, as well as improved learning and memory in the aged mice (4).

Another study shows the effects of blood factors caused by exercise on neurogenesis and cognition in the aged brain (20). These results demonstrate that circulating blood factors in plasma from exercised aged mice are able to transfer the effects of exercise in neurogenesis and cognition to sedentary aged mice. Moreover, they show that some molecules in plasma can improve cognitive function in aged mice. Because in this study both the donors and recipients are aged, these findings suggest that exposure to exercise-induced factors, instead of those associated with younger age, can improve cognitive function (20).

The effects of plasma transfusion from young mice, exercised for 3 months have been studied to investigate if it could improve cognitive functions in an AD model of 12-month-old mice with AD pathology (21). Results from tests of spatial learning and memory, long-term memory, tau proteins, synaptic proteins, mitochondrial function, apoptosis, neurogenesis, and more, suggests the exposure of AD mice to plasma from exercised mice has positive effects on cognitive function (21). Mechanistically, this has been linked to the improved neuroplasticity and mitochondrial function, and suppressed apoptosis. The study hence shows

that exercised plasma can have a protective function on cognitive dysfunction and neural circuits associated with AD (21).

In addition, the “runner plasma” collected from voluntarily running mice and infused into sedentary mice has been found to reduce baseline neuroinflammatory gene expression and experimentally induced brain inflammation. These findings demonstrate that the effects of anti-inflammatory exercise factors are transferrable (22).

1.4.2 Transgenic rat models of Alzheimer’s disease

Rodent models help scientists to elucidate the underlying disease mechanisms of AD, and the results from these studies are starting to uncover the neurobiological basis of AD (23).

Rodent models can also be used to test the effects of different therapeutic drugs and interventions. Both mice and rats are used in research, but living rats and their collected tissues, are easier to handle due to their larger size. The rat brain also has a highly similar structure and functions to the human brain, which makes rats a good non-human model for use in AD research (24).

The transgenic rat models can give a picture of how AD would look like in humans, even though they can’t fully mimic the human AD pathology (23). The cause of the sporadic form is unknown, therefore the rodent models used in research represent the genetic form of the disease.

The most common way to generate transgenic models of AD is to make the animals overexpress mutated APP, the human gene that encodes amyloid precursor protein. These rats are referred to as McGill-R-Thy1-APP, and express a transgene with two mutations of this gene associated with early-onset AD. These mutations are the Indiana (V717F) mutation and the Swedish (KM670/671NL) double mutation. The transgene is regulated by the murine Thy1.2 promoter so that the expression increases with aging of the rats. The McGill rats display intracellular A β accumulation, and increased behavior deficits correlating to the higher A β accumulation. After 6-8 months it is possible to detect the first A β plaques in the hippocampus (25).

1.5 The ExPlas study

A research team at Cardiac Exercise Research Group (CERG) is working on a project called ExPlas. The ExPlas study investigates if the progression of AD in the human brain could be prevented or slowed down through exposure to plasma from young, exercised donors (ExPlas, for exercised plasma).

In the ExPlas preclinical study, plasma from young, exercised donor rats is used to treat older McGill-R-Thy1-APP rats with AD-like pathology (Figure 4). The research group hypothesized that if they inject the young plasma intravenously into the old rat, the “new and healthy” plasma would slow down or prevent the progression of AD pathology, such as the accumulation of A β peptides into plaques and the state of the microglial cells, as they are thought to activate in response to the accumulation of A β (8).

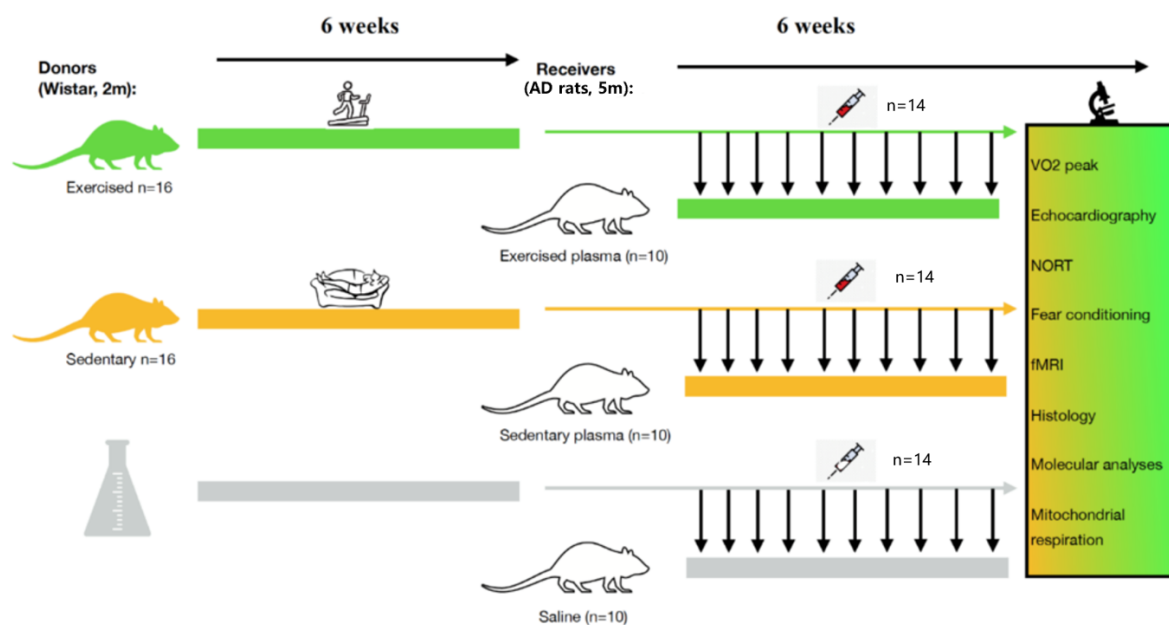


Figure 4. Overview of the preclinical ExPlas study design. 2 months old Wistar donor rats were divided into two groups: exercised rats and sedentary rats. After a period of 6 weeks, Wistar donor rats donated plasma, that was injected into the AD rats' tail vein. The 5 months old AD rats received either exercised plasma, sedentary plasma, or saline (control group). Various tests, including assessment of cardiorespiratory fitness, cognitive functions, cardiac function, and brain structure were done before and after the treatment period. Adapted and modified from CERG/ ExPlas study.

1.6 Immunohistochemistry

Immunohistochemistry (IHC) is a technique that exploits the interaction between antigens (Ags) and antibodies (Abs), and that can be well used on brain tissue sections to assess effects of treatment on various aspects related to AD pathology. Using the technique, Ags of interest present in cells and tissues can be localized and detected by specific corresponding Abs, which is appropriate in clinical diagnostics in anatomic pathology, for example, to assess and detect predictive and prognostic biomarkers (26).

1.6.1 Antigen-antibody interactions

Potential Ags are proteins, carbohydrates, nucleic acids, lipids, or other molecules presented in cells and tissues. The region of the Ags that is recognized by Abs is termed an epitope and is a unique structure of the antigen (Ag) molecule (27).

In contrast, Abs, also called immunoglobulins, are glycoproteins that comprise two heavy- and two light polypeptide chains (27). The antibody (Ab) structure is made up of two functional domains referred to as Fab- and Fc- domains, that together constitute a structure that resembles the letter Y. The “arms” of the Y are termed the Fab- domain and the Ag-binding site, also called paratope, is located on the terminal end on each of these “arms” (Figure 5). The paratopes are made up of variable amino acid sequences that are responsible for Ag-binding and hence determines the Ag specificity of the particular Ab. This means that different Abs recognize different epitopes on different Ags (27,28).

The Fc-domain makes up the “tail” of the Y, and like the Fab-domain, this region consists of a unique structure. This allows other Abs that are directed against the Fc-domain, to recognize and bind to this part of the Ab, which is utilized by indirect detection of Ags, described further below (28).

Monoclonal Abs that are used in research and clinical laboratory diagnostics test such as molecular immunology investigations, are products of a single B cell clone produced in the laboratory. This gives them a unique specificity that allows them to only recognize and bind specifically to a single epitope on an Ag (29).

If a paratope recognizes its corresponding epitope, it binds specifically to it, resulting in an Ag/Ab complex (Figure 5). Presence of the Ag, can then be visualized and detected by using immunofluorescence techniques (30).

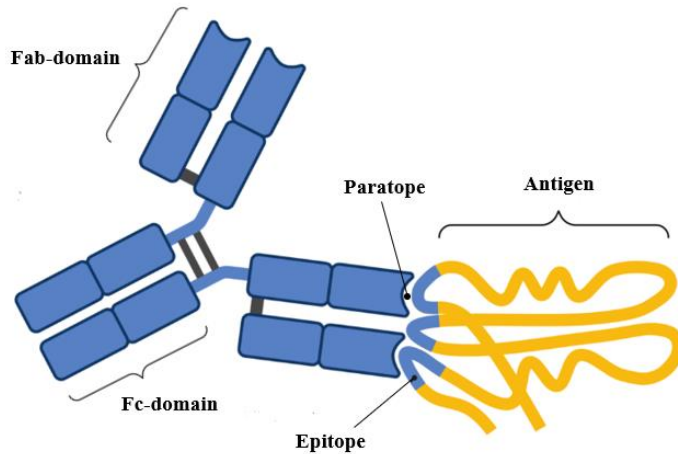


Figure 5. Illustration of an antigen/antibody complex, showing the structures Fab-domain, Fc-domain and paratope on an antibody (blue), and the epitope on an antigen (yellow). Adapted and modified from *sml.sn.no* (31).

1.6.2 Heat-induced antigen retrieval

For diagnosis, IHC is usually performed on formalin-fixed tissues. During formalin-fixation, protein cross-links are formed to retain the tissues stability and structure during storage (26). These cross-links will mask the Ag sites, thus preventing the Abs from reaching the Ags. To facilitate Ag/Ab binding, the tissue must be unmasked before IHC staining, to make the Ag sites available. This unmasking is referred to as antigen retrieval and could be mediated by enzymes or heat (32). The heat-mediated method is mostly preferred and is specifically called heat-induced antigen retrieval. The tissue is incubated in a retrieval solution and can be heated using, for example, microwave ovens or water baths (26,32).

1.7 Immunofluorescence

Immunofluorescence is a widely used technique in both scientific research and clinical laboratories. The technique uses fluorescently-labeled Abs which are directed against and bind to corresponding Ags. By using fluorescence microscopy the fluorescence signal can be detected and quantified, and in this way, visualize if and where the Ag/Ab reaction has occurred, thus where the Ag of interest is located in the tissue (28).

The Ags of interest can be directly detected by using a single fluorophore-labeled Ab, or indirectly through a fluorophore-labeled secondary Ab. The indirect method is a two-step technique, the primary Ab and the secondary Ab are added separately. In the first step an unlabeled primary Ab binds to the corresponding Ag in the tissue. When a fluorophore-labeled secondary Ab is added, the secondary Ab (Fab-domain) binds to the Ag-bounded primary Ab (Fc-domain) (Figure 6). The direct method is specific and effective since the technique requires one incubation, compared to the indirect method that is more complicated and time consuming. However, the indirect method is more sensitive, because several labeled secondary Abs can bind to a single primary Ab, thus providing a stronger fluorescence signal (28).

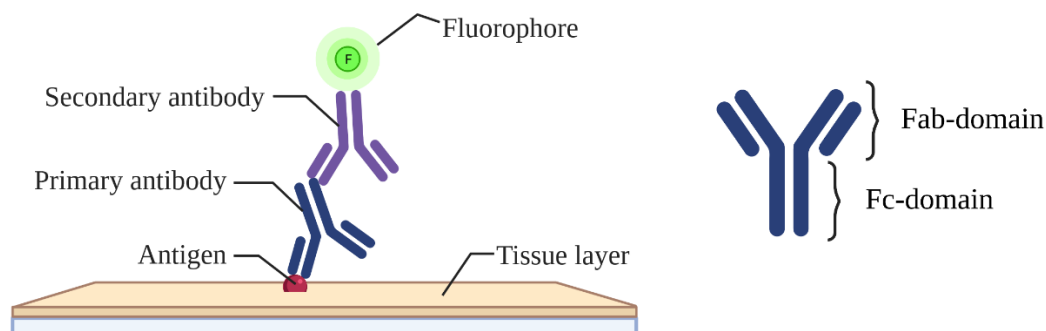


Figure 6. Illustration of an indirect fluorescence method. The Fab-domain on a fluorophore-labeled secondary antibody is bound to the Fc-domain on a primary antibody, that is attached to an antigen in the tissue. Created with [BioRender.com](https://www.biorender.com).

1.7.1 Fluorescence microscopy

Fluorescence microscopy is an important imaging approach for studying and detecting desired cellular parameters, including both endogenous autofluorescence and exogenously fluorophore-labeled molecules. It is preferably used to visualize immunofluorescence for detection of Ag/Ab complexes. The main advantage of fluorescence microscopy is the ability to provide great images with high quality, by using several filters, that for example reduce background interference (33,34).

Fluorescence microscopy is based on the fluorescence technique, where high-energy light irradiates and excites fluorophores in the sample, causing fluorescence light with less energy to be emitted and detected. LED light is commonly used as a light source in fluorescence microscopy. The LED light will emit photons (light) that will pass through an extraction filter before reaching the sample (35). The light is filtered so light with certain wavelengths that are known to excite the electrons in the fluorophore(s), passes through, before the light hits a dichroic mirror which further centers the light towards the sample. The sample (fluorophore) absorbs the light, and the electrons go to a higher energy state (excitation). When they reach this state, they quickly return to the ground state, and energy is released as photons (emission). The sample starts fluorescing, and this fluorescence (emission light) returns through the dichroic mirror, and then an emission filter. The emission filter blocks out any excitation light, so that only emission light reaches the detector. The emission light has lower energy, and longer wavelength than the original excitation light because of energy loss in the process (33–35). The emission light (fluorescence signal) is detected at a specific wavelength, the detection itself is independent of a color, and with a setting on the microscope it can be decided which color (pseudo-color) the visualized signal will be. Figure 7 shows a basic overview of a fluorescence microscope.

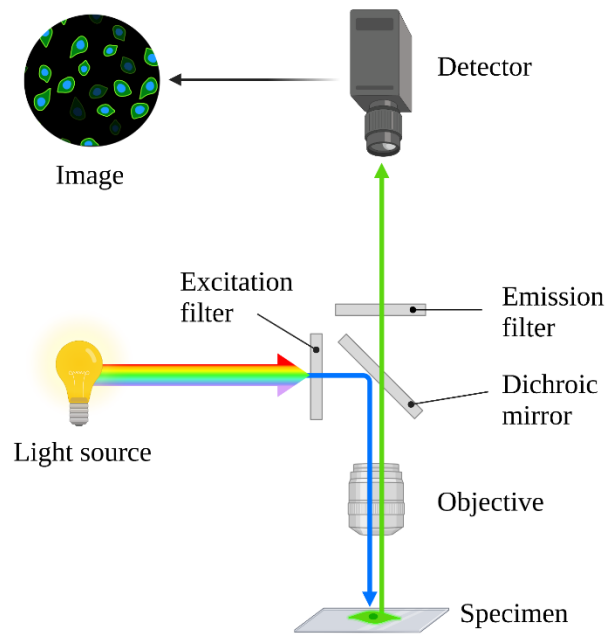


Figure 7. A basic overview of the light path and the components of a fluorescence microscope. Created with [BioRender.com](https://www.biorender.com).

Photo bleaching is a limitation of fluorescence microscopy. Fluorophores have limited number of excitation cycles so their capacity to fluoresce tends to bleach out over time during illumination. This is an irreversible process, the ability to detect the signal from the sample can be lost (33).

Autofluorescence is also a limitation of the technique. Endogenous fluorophores in the tissue can excite and emit light that the filters might be unable to get rid of. The light could be detected, and then introduce artefacts and interfere the image output (33,36). This autofluorescence could originate from mitochondria and lysosomes (37).

1.7.2 Confocal microscope

Confocal microscopy is a specialized fluorescence imaging technique, that uses lasers as light source. In a fluorescence microscope, every dyed molecule in the tissue will be stimulated, including those in out-of-focus planes. It is therefore not possible to have control of which plane the detected signal is emitted from (33). One of the advantages of the confocal microscope is the use of a pinhole, which filters out the out-of-focus light, by removing unwanted light above and below the focal plane. This makes it possible to know which plane the emitted light is from, which makes optical sectioning possible for three-dimensional

reconstructions of imaged samples, in addition to provide great images with high resolution and contrast in thick tissues (33,38,39).

Photo bleaching is a major problem in confocal microscopy compared to regular fluorescence microscopy. This because high-energy light is focused to a smaller point, which results in a higher degree of bleaching (33).

1.8 Aim of this project

The main aim of this Bachelor's thesis project was to examine if plasma from young exercised donor rats affects the accumulation of A β , and the activity of microglial cells in Alzheimer's disease rat models, by using indirect immunofluorescence and confocal microscopy. Brain tissue from the following three groups of rats was analyzed; 1. untreated wild-type rats (wild-type rats), 2. untreated AD rats (AD rats) and 3. ExPlas-treated AD rats (ExPlas rats).

This project's hypothesis is that ExPlas rats have less A β accumulation and less activated microglial cells in the subiculum region, compared to AD rats, and that ExPlas rats have more similarities to wild-type rats. The specific questions to examine the main aim in this project are following:

1. Is there a difference in A β accumulation between the three groups?
2. Is there a difference in activation of the microglial cells between the three groups?
3. Is there a connection between A β accumulation and microglia activation?

2.0 Materials and methods

2.1 Project design

In this project, immunofluorescence staining was performed on free-floating rat brain tissue, collected from untreated wild-type rats (n=3), untreated AD rats (n=3) and ExPlas-treated AD rats (n=4, from the preclinical ExPlas study). All the analyzed rats were 6 months old at the time of collection. ExPlas rats were compared with wild-type rats and AD rats. Two free-floating brain sections per rat were stained. In addition, one section of positive control and one section of negative control were included, to ensure the quality of the staining processes. An overview of the age and number of rats in each group of the used rat models is described below in table 1.

All the brain tissue used in this project had been collected from rats transcardially perfused with 4% paraformaldehyde (PFA), serially sectioned to 40 μ m slices, and stored in 10% DMSO for 2 – 4 years, at +4 °C. The DMSO solution has been described to be the best for long time storage solution to preserve the tissue (40). More detailed description of the ExPlas-treatment and tissue collection are provided in Appendix I.

Table 1. An overview of the samples/ rat models used in this project, including age and number of rat models in each group and the controls. The 8 controls include 4 positive and 4 negative stained controls. A more detailed table is shown in Appendix II.

	Age (months)	Number (n)
Wild-type rats	6	n=3
AD rats	6	n=3
ExPlas rats	6	n=4
Controls	12	n=8

Immunofluorescence was used for detection of A β and microglia in the subiculum region of the brain. An indirect immunofluorescent protocol, utilizing a two-step technique was used. Monoclonal primary unlabeled Abs specific to the Ags of interest, 42 amino acids long A β peptides and microglia-specific cytosolic protein called ionized calcium-binding adapter molecule 1 (Iba1), were used in combination with compatible, fluorophore-labeled secondary Abs, to allow visualization of A β peptides and microglial cells in the subiculum region of the brain with confocal fluorescence microscopy (28).

2.2 Rat models

All experimental procedures in the ExPlas preclinical study that involved rodents have been approved by the Norwegian food and safety authority (FOTS ID: 11740).

The ExPlas rats and the AD rats used in this study were male McGill-R-Thy-1-APP transgenic rats, which express human APP with the Swedish and Indiana mutation, controlled by murine Thy1.2 promoter (provided by Professor Menno Witter at Kavli Institute for Systems Neuroscience at the Centre for Neuronal Computation at NTNU Trondheim) (13). The wild-type rats and the exercised plasma donor rats were male, non-transgenic Wistar rats.

2.3 Immunofluorescence staining protocol for amyloid-beta and microglia

The free-floating brain tissue used in this project were stained according to a protocol attached as appendix III.

In the first step of the protocol, heat-induced antigen retrieval was used to unmask Ags from formalin-mediated cross-links. The free-floating brain sections were divided into brain cups containing preheated Sodium Citrate buffer (10mM Sodium Citrate, 0,5% Tween, pH 6.0) and kept in an 80 °C water bath for 45 minutes. After incubation, the sections were rinsed in Tris-buffered saline (TBS, pH 8.0) for 3 x 10 minutes, to remove the Sodium Citrate buffer. The brain sections were incubated in 10% goat serum (Invitrogen, Cat# 10000C, LOT #VH307567) in TBS-Triton X-100 (TBS-Tx 0,5%, pH 8.0) for 60 minutes, to saturate the tissue and prevent non-specific background staining. Two different unlabeled primary Abs, one for each Ag of interest were added; Mouse monoclonal antibody to A β 1-42 (12F4) (1:500 in TBS-Tx, Biolegend, Cat#805501, RRID: AB_10732141, LOT #B291738) and Rabbit monoclonal antibody [EPR16588] to Iba1 (1:2000 in TBS-Tx, Abcam, Cat#

ab178846, RRID: AB_2636859, LOT #GR3335980-4). The primary Abs were allowed to bind the Ags and form the Ag/Ab complexes upon overnight incubation at +4 °C.

The following day the sections were rinsed in TBS-Tx for 3 x 10 minutes, to wash off the unbound primary Abs in the solution. Two fluorophore-labeled secondary Abs were added and incubated for 60 minutes; Goat Anti-Mouse IgG H&L (Alexa Fluor 488) antibody (1:667 in TBS, Abcam, Cat# ab150113, RRID: AB_2576208, LOT #GR3419505-1) and Goat Anti-Rabbit IgG H&L (Alexa Fluor 594) antibody (1:500 in TBS, Abcam, Cat# ab150080, RRID: AB_2650602, LOT #GR3401492). The fluorophore-labeled secondary Abs were bound to the primary Abs to detect the Ags of interest. To prevent the fluorophore (and thus the signal) from getting bleached, the sections were covered with aluminum foil under this incubation and the next steps in the procedure.

After secondary Ab incubation, the sections were rinsed in TBS 2 x 5 minutes, before the cell nuclei were stained by incubation in DAPI solution (1:2000, Abcam, Cat# ab228549, LOT #GR3336573-3), followed by a rinse-step for 5 minutes in TBS. In the last step of the process the sections were transferred on glass slides (*Epreidia* Superfrost Plus Adhesion Microscope Slides) while floated in TBS, and dried for at least 30 minutes before adding Vectashield Antifade Mounting Medium (Lot number ZH0804) and a coverslip. The mounting medium acts as preparation that maintains the tissue, so it could be preserved longer, and amplifies the fluorescence signal. The coverslip was sealed on the glass slide using nail polish.

2.3.1 Positive and negative controls

The positive and the negative controls used were 12 months old AD rats (McGill-R-Thy1-APP model). These samples were both stained according to the staining protocol (Appendix III), simultaneously with the brain section samples, except that the negative control was not incubated with the primary Abs. The positive control was incubated with both primary Abs and secondary Abs.

2.3.2 Changes and modifications of the protocol

For protocol optimizing, a preadsorbed fluorophore-labeled secondary Ab for A β ; Goat Anti-Mouse IgG H&L (Alexa Fluor 488) preadsorbed (1:1000 in TBS, Abcam, Cat# ab150117, RRID: AB_2688012, LOT #GR3398339-3) was performed on one brain section from each of

the 10 rats included in this project, otherwise using the same protocol. This was done to exclude the possibility of similarities in rat and mouse IgG resulting in unspecific binding, since the preadsorbed secondary Ab should be more specific and therefore show less unspecific binding. The difference between this preadsorbed secondary Ab compared to the secondary Ab (Goat Anti- Mouse IgG H&L (Alexa Fluor 488)) used in the original protocol, is that the preabsorbed Ab has been specifically produced to show reduced cross-reactivity to rat IgG (41).

2.4 Detection and quantification

The tissue was imaged using the Zeiss LSM 510 Pascal Confocal microscope (Zeiss, Germany) with the objective lens Plan-Neofluar 40x/1,3 Oil DIC. Using the microscope, the fluorescent signal can be specifically visualized and detected in three-dimensional tissue sections (in the 40 μm thick tissue sections). To detect the secondary Abs, the fluorophores Alexa Fluor 488 and Alexa Fluor 594, were excited with the 488 nm and 561 nm laser, respectively. Signal from these fluorophores was selected to be visualized as green (A β) and red (microglia).

2.4.1 Image acquisition and skeleton analysis

Analyses of microglial count and morphology were performed on four z-stack images of subiculum from each brain (images of subiculum on the right and left sides in two brain sections) utilizing Fiji software and a script that was tailored following a previously described protocol for morphological analyses (42). The script first processed the raw images into single channel stacks. Microglial cells were manually counted from the stack images with the help of the Cell Counter plugin to mark all counted cells to ensure no double counting. The stacked images with Iba1 staining were further processed for enhanced visibility of microglial processes and their branching prior to thresholding and skeletonizing the image. Skeleton analysis was then run with circle pruning of the shortest branch and detailed information about branch count, branch length, and the number of endpoints was collected for statistical analyses with the criteria described in Figure 8.

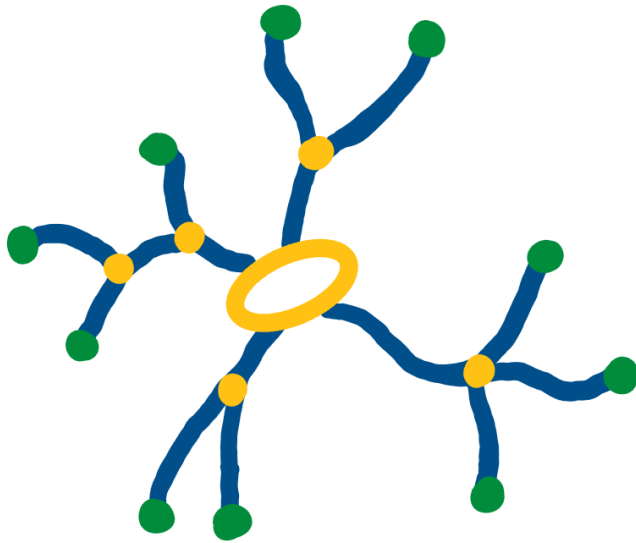


Figure 8. Illustration of a microglia cell. End-point pixels are displayed in green, slab voxels in blue (branches) and junction voxels in yellow, the soma of the cell is counted as a junction voxel. Illustration by Jenny Bakken.

2.4.2 Statistical analyses

All statistical analyses were performed using IBM SPSS Statistics software version 28.0.1. Kruskal-Wallis 1-way ANOVA were used to compare the groups. Only $p < 0.05$ were considered statistically significant.

3.0 Results

The preclinical ExPlas study investigated whether exercised blood can influence AD, by preventing or reducing its development. A β accumulation in the subiculum region of the brain is a hallmark of AD. It is in this region where the AD rat model first expresses A β plaques (13), and the presence of A β accumulation is regarded to be related to the status of microglia activity. To compare the differences of A β accumulation and microglial cells in the subiculum region between the three groups, in addition to investigating the connection of A β accumulation and microglial cells, immunofluorescence and statistical analysis were performed on brain tissue sections from wild-type rats, AD rats and ExPlas rats.

3.1 Amyloid-beta and microglial cells combined

The wild-type rat (Figure 9A), AD rat (Figure 9B) and ExPlas rat (Figure 9C) all showed positive staining for A β accumulation (green) and microglial cells (red) in the subiculum region. The “positive” staining for A β in wild-type rat was unexpected.

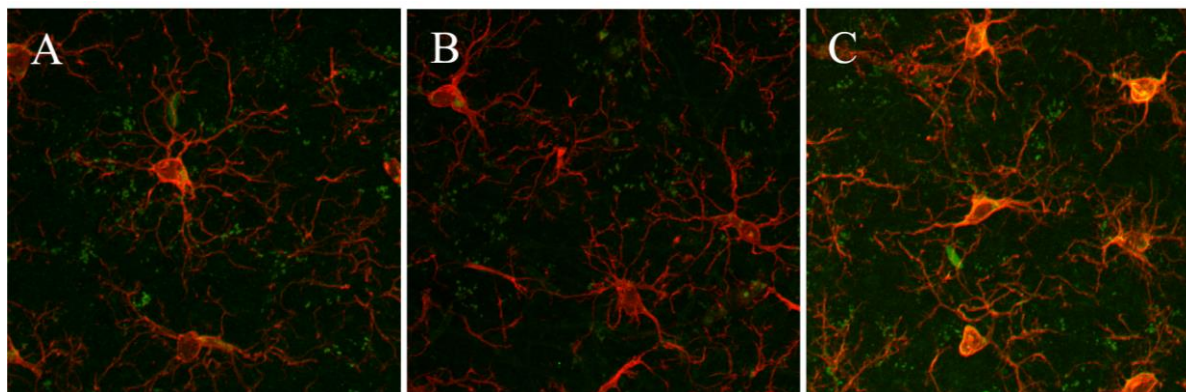


Figure 9. Images of the subiculum region in rat brains of one selected rat from the three different groups, showing signals of A β (green) and microglial cells (red). A: wild-type rat, B: AD rat, C: ExPlas rat. 40x images were taken with Zeiss LSM 510 Pascal Confocal. The images of A β accumulation and microglial cells were combined utilizing Fiji software.

3.2 Microglial cells

To visualize the morphology of microglial cells, microglial protein Iba1 was stained with specific Abs and detected using Zeiss LSM 510 Pascal Confocal microscope. A typical microglial cell visualized in the subiculum region from a wild-type rat contained a lot of branches (Figure 10A). A typical microglial cell in the AD rat brain showed, in contrast less branches (Figure 10B). A typical microglial cell in the brain of an ExPlas rat had more similarities to the microglial cell in the wild-type rat (Figure 10C), considering the number and length of the branches.

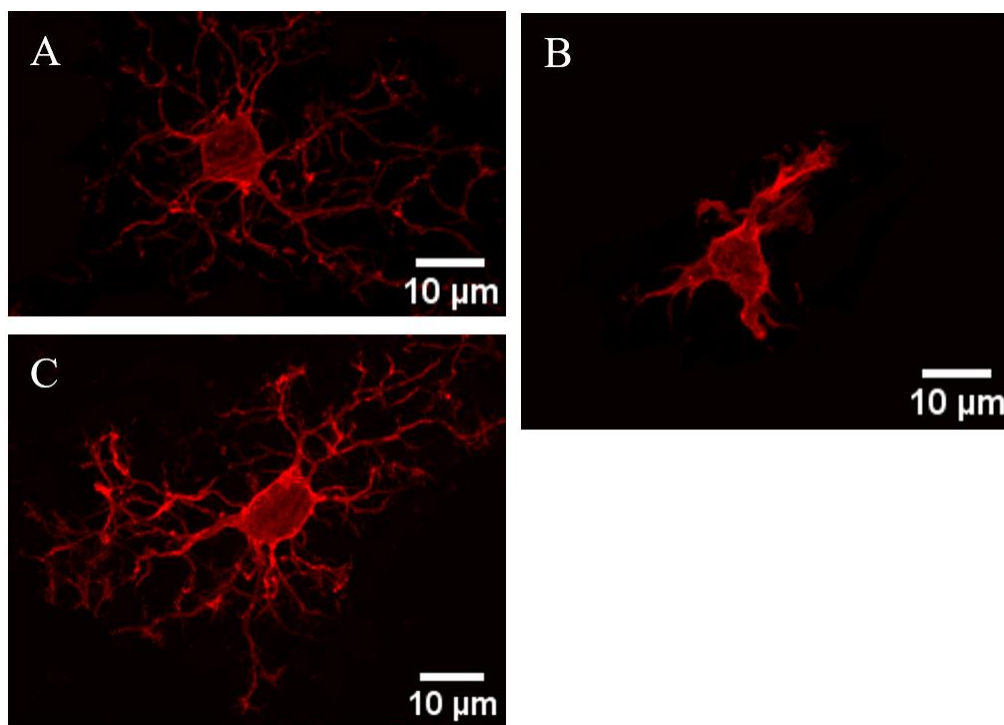


Figure 10. Examples of microglial cells in the subiculum region of the brain, of one cell from each group. A: A microglial cell in a wild-type rat, B: A microglial cell in an AD rat, C: A microglial cell in an ExPlas rat. 40x images were taken with Zeiss LSM 510 Pascal Confocal and cropped to show a single microglial cell.

All the three groups; wild-type rat (Figure 11A), AD rat (Figure 11B), and ExPlas rat (Figure 11C) showed microglial cells in the subiculum region.

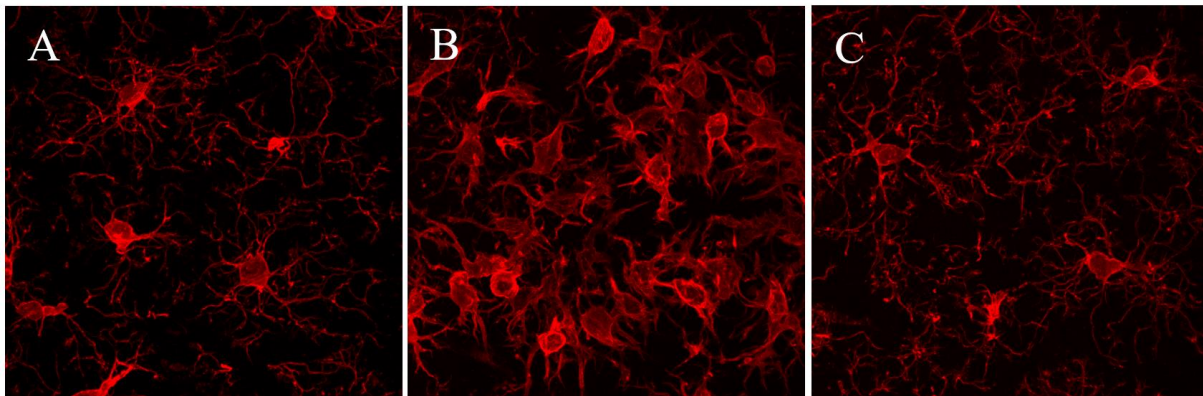


Figure 11. Images of the subiculum region in rat brains of one selected rat from the three different groups, showing microglial cells (red). A: wild-type rat, B: AD rat, C: ExPlas rat. In the AD rat (B), the cells have clustered, migrated to imaged area. 40x images were taken with Zeiss LSM 510 Pascal Confocal.

All statistical analysis on the microglial cells were analyzed by using IBM SPSS software and Kruskal-Wallis 1-way ANOVA.

Total number of microglial cells in the imaged region of the subiculum was manually counted from 40x confocal images. There were more microglial cells in the ExPlas brains compared to the brains of the wild-type rats (Figure 12, $p=0.008$). There were no significant differences between other groups in the number of microglia.

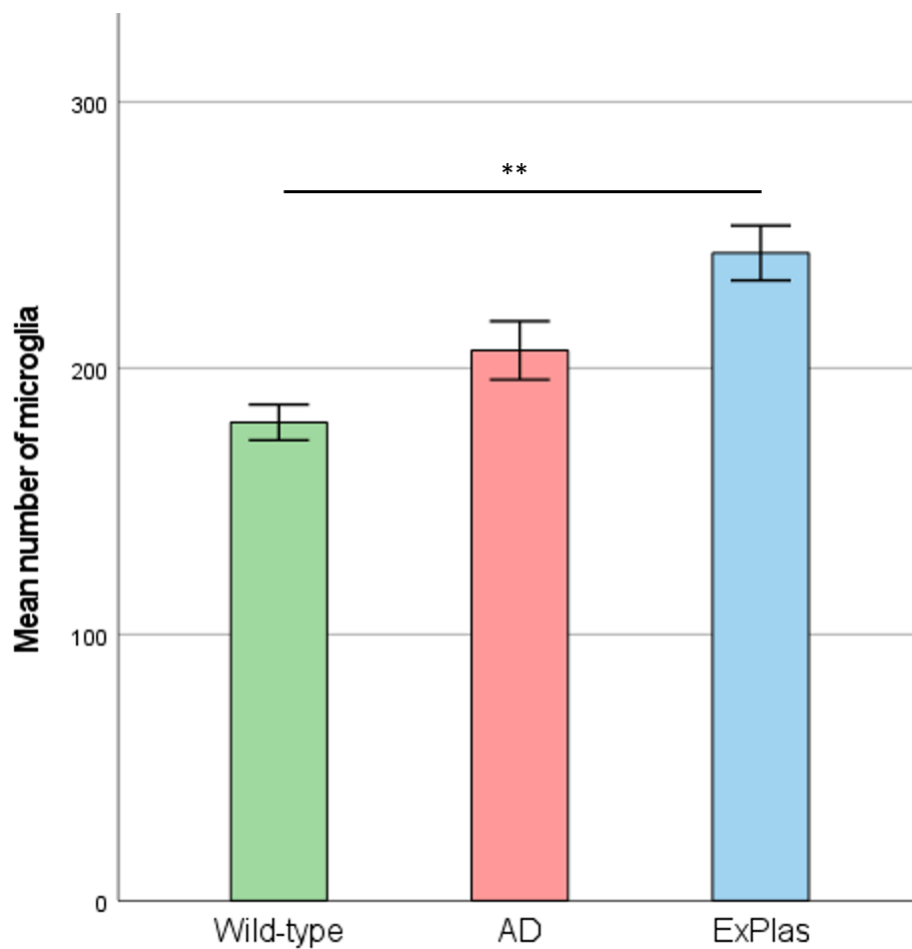


Figure 12. Total microglial count in the region of interest within the subiculum of wild-type rats (green), AD rats (red) and ExPlas rats (blue). Total number of microglial cells was manually counted from four individual 40x confocal images of the subiculum region in the brain ($n=3-4$ in each group). All data are presented as mean \pm standard error of the mean (SEM), performed using Kruskal-Wallis 1 way ANOVA; $**p=0.008$ (wild-type–ExPlas).

The number of branches of the microglial cells in imaged region of the subiculum was automatically counted from 40x confocal images. The number of branches per microglia showed no significant differences between any of the groups (Figure 13).

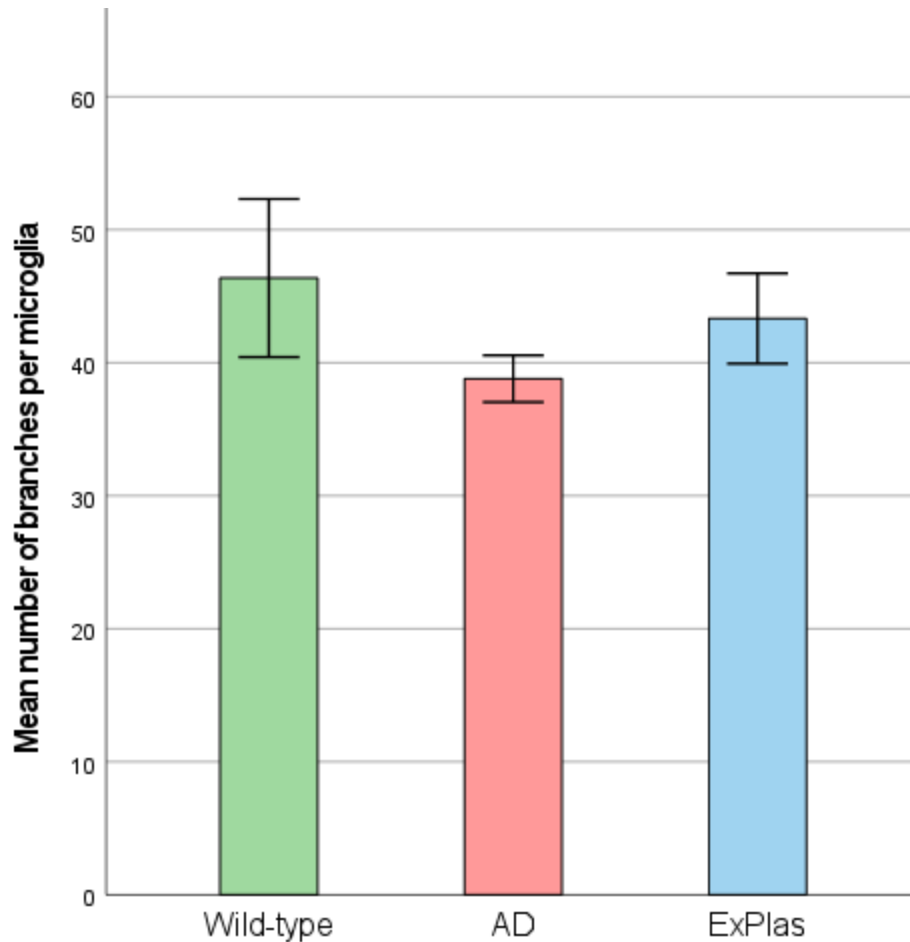


Figure 13. Total number of branches per microglial cell in the region of interest within the subiculum of wild-type rats (green), AD rats (red) and ExPlas rats (blue). Total number of branches was automatically counted from four individual 40x confocal images of the subiculum region in the brain ($n=3-4$ in each group), then the mean number of branches were divided by the manually counted number of microglial cells. All data are presented as mean \pm standard error of the mean (SEM), performed using Kruskal-Wallis 1 way ANOVA.

The branch length of the microglial cells in the imaged region of the subiculum was automatically measured from 40x confocal images. The wild-type rat and the ExPlas rat displayed longer branches per microglial cells compared to the AD rat (Figure 14, $p=0.031$, $p=0.040$, respectively).

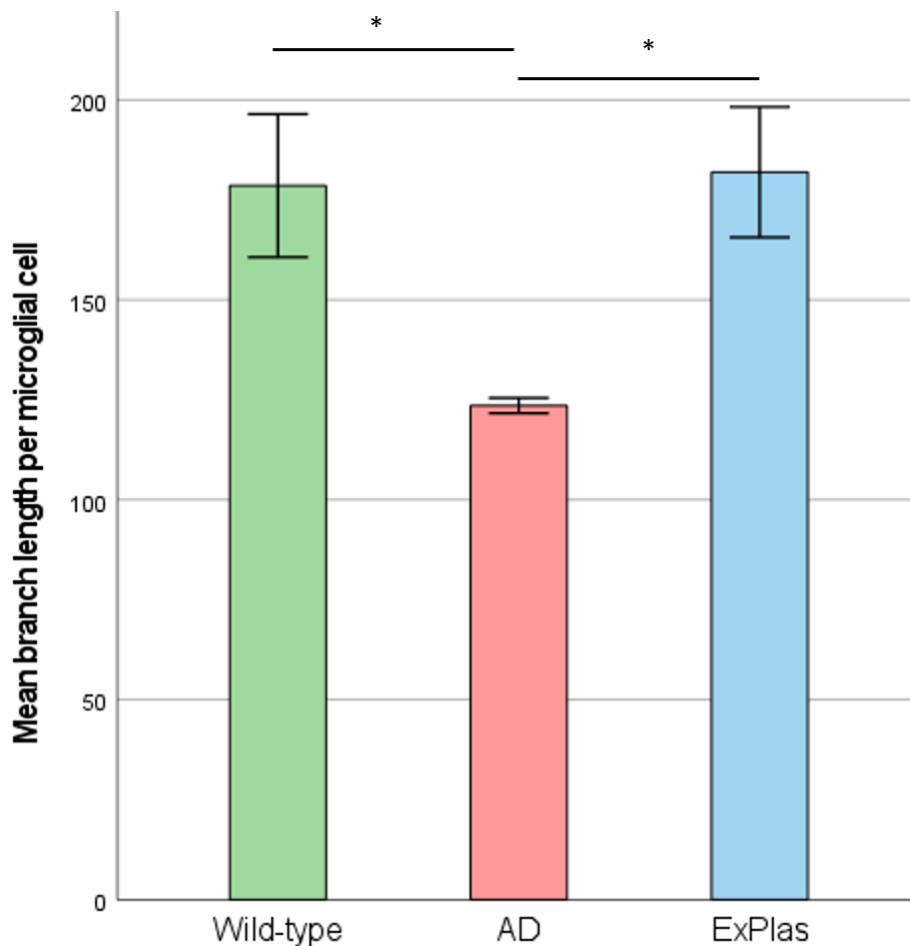


Figure 14. Total length of all counted branches per microglial cell in the region of interest within the subiculum of wild-type rats (green), AD rats (red) and ExPlas rats (blue). Total branch length was automatically counted from four individual 40x confocal images of the subiculum region in the brain ($n=3-4$ in each group), and then divided by the manually counted number of microglial cells. All data are presented as mean \pm standard error of the mean (SEM), performed using Kruskal-Wallis 1 way ANOVA; $*p=0,031$ (Wild-type-AD), $*p=0,040$ (AD-ExPlas).

The number of endpoints of the microglial cells in the imaged region of the subiculum was automatically measured from 40x confocal images. The ExPlas rat displayed more endpoints per microglial cell compared to the AD rat (Figure 15, $p=0.040$).

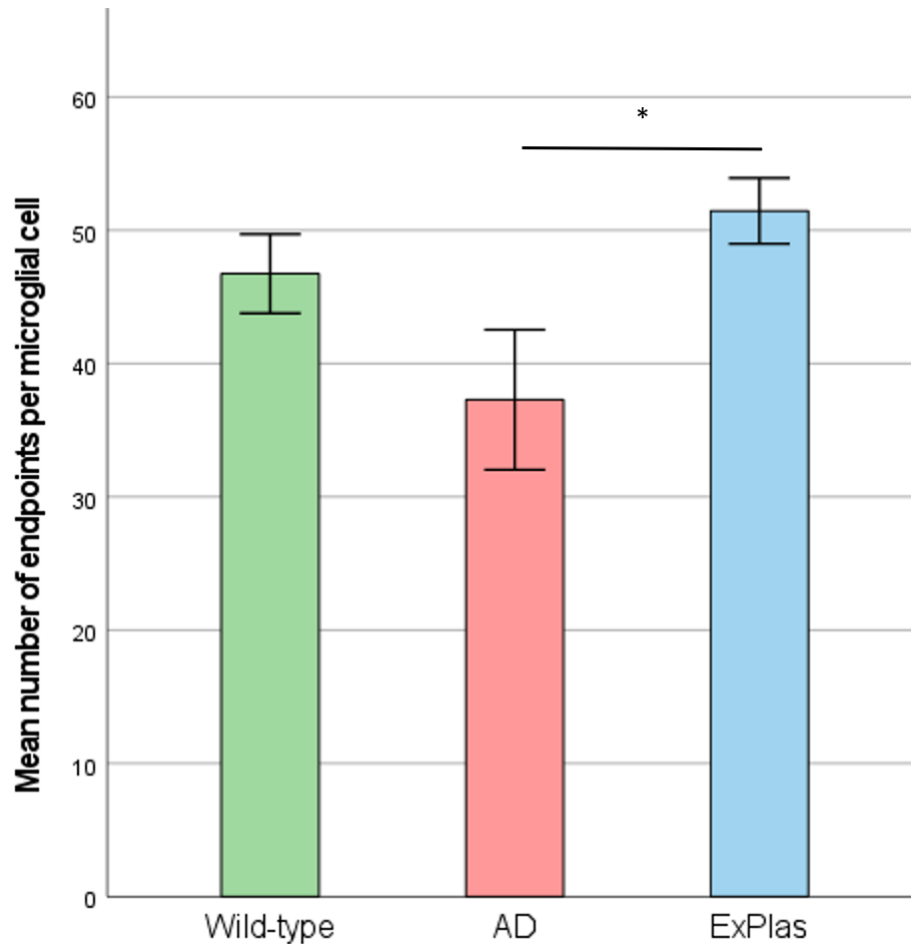


Figure 15. Total number of endpoints per counted microglial cell in the region of interest within the subiculum of wild-type rats (green), AD rats (red) and ExPlas rats (blue). Total number of endpoints was automatically counted from four individual 40x confocal images of the subiculum region in the brain ($n=3-4$ in each group) and divided by the manually counted number of microglial cells. All data are presented as mean \pm standard error of the mean (SEM), performed using Kruskal-Wallis 1 way ANOVA; $*p=0,040$.

3.3 Amyloid-beta

To visualize A β accumulation, A β peptide was stained with specific Abs and detected using Zeiss LSM 510 Pascal Confocal microscope. The wild-type rat (Figure 16A), AD rat (Figure 16B), and ExPlas rat (Figure 16C) showed positive A β staining, similar to the signal also detected in the control tissue, in the subiculum region. Unlike the wild-type rat, AD rat and ExPlas rat showed some “true” signal of A β accumulation, pointed at by white arrows (Figure 16B and 16C).

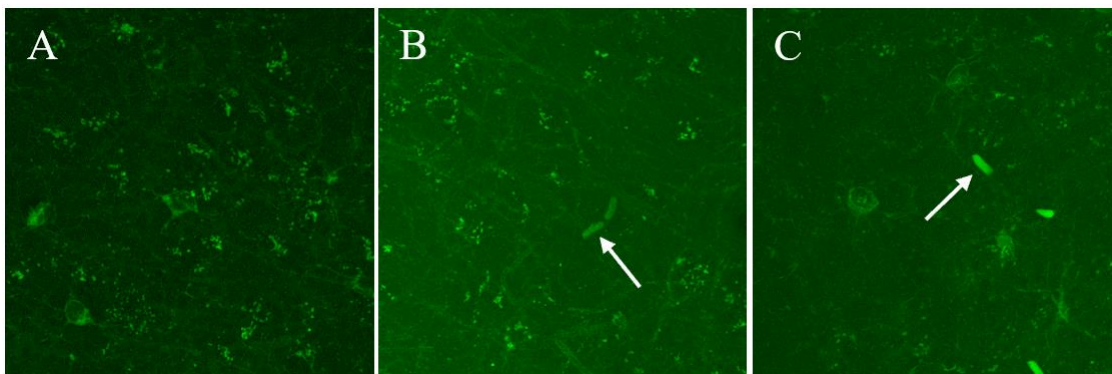


Figure 16. Images of the subiculum region in rat brains of one selected rat from the three different groups, showing signals of A β . A: wild-type rat, B: AD rat, C: ExPlas rat. A β signals in the wild-type rat were unexpected. A β accumulation is pointed at by with arrows in AD rat and ExPlas rat. 40x images were taken with Zeiss LSM 510 Pascal Confocal.

3.4 Controls

During staining, controls were included, both a negative control (Figure 17A) and a positive control (Figure 17B) for both A β and microglial cells. The negative controls showed partly similar signal for A β as the positive control.

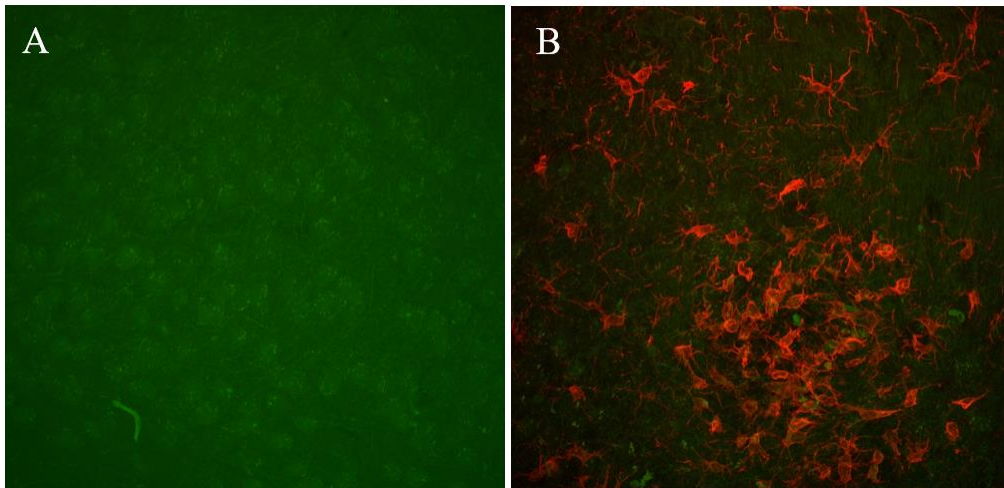


Figure 17. Images of the negative and positive controls for both A β and microglial cells, in the subiculum region. A: negative control, B: positive control. 40x images were taken with Zeiss LSM 510 Pascal Confocal. The control of microglial staining is valid; the negative control showed no microglial cells, and the positive control did. The negative control is showing “positive” A β staining, partly similar to that in the positive control; the control is not valid.

Negative control for A β and microglial cells, showed signal for A β (Figure 18) also when stained with the new preadsorbed secondary Ab.

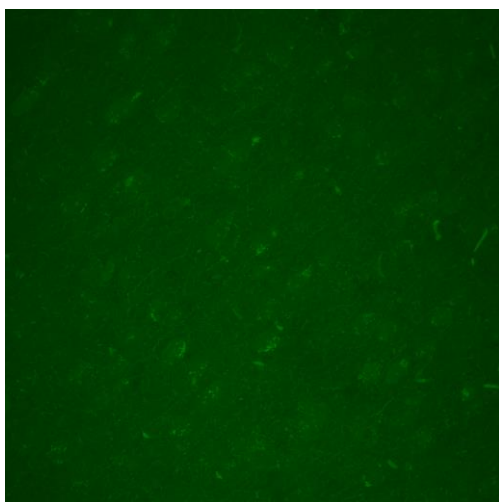


Figure 18. Images of the negative control for both the A β and microglial cells in subiculum region. A β were stained with the new secondary Ab (Goat Anti-Mouse IgG H&L (Alexa Fluor 488) preadsorbed). 40x images were taken with Zeiss LSM 510 Pascal Confocal. The negative control is showing “positive” A β staining; the control is not valid.

4.0 Discussion

Studying microglia and A β can inform about pathological changes in AD brain. The microglial cells are thought to be capable of surveying the brain for A β , and if discovered, they may cluster around it for phagocytosis. The results of this project show that exercised plasma had an effect on the activation state of the microglial cells, when compared with the wild-type rats, and the AD rats. The ExPlas rats had more similarities to the wild-type rats than to the AD rats. The results for A β could not be trusted, or analyzed, due to presumed high autofluorescence and low level of true signal, and therefore the potential differences of A β accumulation and the connection between microglial cells and A β could not be assessed, between the three groups. All staining of microglia was instead successful and allowed detailed analyses.

4.1 Microglial cells

The most essential functions of the microglial cells are removing damaged neurons and debris, immune surveillance and maintaining the synaptic plasticity. The microglial cells can be activated in response to accumulation of AD pathology. An activated microglial cell has less and shorter branches than an inactive (surveying) cell. When a microglial cell has more branches, it also has more endpoints (14,15). These changes are also depicted in the exemplary figures of single microglial cells from a rat of each group (Figure 10). The morphology of microglial cells in a wild-type rat had many and long branches (Figure 10A), suggesting the cells are inactive. The microglial cells in the AD rat, in contrast, had shorter and fewer branches (Figure 10B). This indicates that the cells were activated. The microglial cells in the ExPlas rat (Figure 10C), had more similarities to the microglial cells in the wild-type rat, when comparing the cells morphology.

Similarly, the exemplary images (Figure 11) show microglial cells in the subiculum region of one individual from each of the three different groups. The wild-type rat image (Figure 11A) shows inactive microglial cells because of the branches. In the AD rat image (Figure 11B) the cells had clustered to one area. The cell morphology was different, showing less and shorter branches in this group, compared to the microglial cells in the wild-type rat. This indicates more active cells, that could mean that the cells were active with removing A β accumulation in the AD rat brain. This explains a possible reason for the visualized cluster (Figure 11B).

The ExPlas rat image (Figure 11C) visualizes more similarities to the wild-type rat image (Figure 11A).

Between-group statistical analyses showed that the ExPlas rats had a significant ($p=0,008$) increased number of microglial cells in the subiculum, compared to the wild-type rats (Figure 12). The cause of this can be that the exercised plasma has stimulated to produce more microglial cells. The analyses also showed that the ExPlas rat had more microglial cells compared to AD rat, but the difference was not significant. The higher number of microglial cells in ExPlas rat compared to the AD rat, could mean that exercised plasma influences the number of microglia.

The mean number of branches per microglia could also have given an indication if the exercised plasma had an effect of the microglia state, but this could not be considered because of the non-significant results between the groups (Figure 13).

There was a significant difference ($p=0,031$, Figure 14) between the branch length per microglial cell in wild-type rats compared to AD rats, with shorter branches in AD rats. This may be expected since $A\beta$ accumulation or plaques are likely in AD rats, and those could activate microglia to a phagocytic stage, where they have shorter branches (as in Figure 10B). There was also a significant difference ($p=0,040$, Figure 14) between ExPlas rats and AD rats. ExPlas rats had longer branches per microglial cell, which indicates that exercised plasma had affected the state of the microglia, to less active. The length of branches in ExPlas rats were quite similar to wild-type rats', which could further indicate that exercised plasma had an effect on the microglia state.

The number of endpoints per microglial cell showed a significant difference between ExPlas rats and AD rats ($p=0,040$, Figure 15). This indicates that exercised plasma treatment changes the microglia morphology.

Various studies have demonstrated that the effects from exposure to exercised young blood are similar to the positive effects that exercise training has on the brain, or more specifically to the hippocampus (20–22). Only one study has reported effects on neuroinflammation (22). Specifically, plasma from running mice was found to reduce expression of inflammation related genes in the brain of mice with induced neuroinflammation (22). These findings are in line with ours, as our results also suggest that exposure to exercised plasma, has positive

effects on the brain. Our results indicates that exposure to young, exercised plasma may reduce the activation of microglial cells.

The results from the statistical analysis combined gives an indication of exercised plasma's effect on the microglia state. The treated ExPlas rats had more similarities to the healthy wild-type rats, than the untreated AD rats. This could indicate that exercised plasma treatment has an indirect effect on the microglial state, in the way that exercised plasma could have prevented A β accumulation or other microglial triggering/activating molecules, in ExPlas rats. A brain with less A β and damage to neurons, could therefore lead to a less active microglial cell (16). The Explas rats had a significantly increased number of microglial cells in the subiculum. More microglial cells could give a better protection against the incidence of AD, since microglial cells are surveilling the area, and potentially phagocytosing A β .

4.2 Amyloid-beta

Unfortunately, the A β results (Figure 16) were not as expected since the images of the wild-type rat (Figure 16A), the AD rat (Figure 16B), and the ExPlas rat (Figure 16C) showed positive staining for A β accumulation. It was not expected to get fluorescence signal in wild-type rats (Figure 16A) since they should not have A β accumulation and plaques. The negative controls (Figures 17A and 18) support this finding because it shows “positive” staining for A β accumulation similar signal to that in positive control (Figure 17B), as well as all other stained tissue (in Figure 9 and 16). The results could not be analyzed because of low contrast between false and true positive signal. Therefore, performing the planned statistical analyses for comparing the A β accumulation between the three groups, was not feasible. These findings indicate that other structures than those of interest had become visible. There could be several reasons for these findings, but non-specific secondary Ab and autofluorescence are two potential reasons that we consider as relevant.

It is essential to make sure that the Ab used are specific enough, to avoid non-specific binding to other components that are not of interest. Monoclonal primary Abs, as used in this project, have a unique specificity that only allows them to bind to a single epitope on an Ag. Due to this, and that primary Abs was not added in the negative control, the problem could most likely be related to the secondary Ab. A new preadsorbed secondary Ab was then tested, because of the unexpected results showing signs of unspecific binding with the previously used secondary Ab. The benefit of using this new Ab is reduced cross-reactivity to rat IgG.

The results showed no improvement, there was still “positive” signal for A β (Figure 18). The specificity of the secondary Ab, in addition to cross-reactivity problems, could therefore most likely be excluded as a cause of “positive” staining.

Autofluorescence may be another cause for the “positive” signal. If this hypothesis is correct, there is something else in the tissue, which is not of interest, that has given fluorescence. Mitochondria and lysosomes are known sources of autofluorescence and based on the localization of “positive” staining inside cells, it looks like this might be the case in our results (37). It is described that tissue should not be stored in PFA for too long, to avoid over fixation that could increase the autofluorescence (44). The rats used in this project were first fixated with 4% PFA, before the brain tissue were collected and left in 4% PFA for 24 hours. If the fixation can be considered as “too long”, this may be another cause of the autofluorescence. Our tissue had been stored in DMSO solution for 2-4 years, and since it is described that the shelf life of the tissue stored in DMSO solution is good for 2 years, it may be that the tissue had been stored for too long, thus been damaged (40). This may therefore also be a possible source of autofluorescence.

In addition to false positive signal, all the tissue including the negative control (Figure 17A) also showed a lot of green background staining. Background staining could be a problem because it makes it hard to separate the A β plaques from the green background. One possible reason for background staining that we have considered as relevant, is that the goat serum could be insufficient. The tissue was incubated with 10% goat serum for 60 minutes to prevent non-specific background staining. If this is the reason for the high level of background staining, it could be fixed by increasing the incubation time or changing to a new blocking agent (45). This could be excluded since this problem could not be seen with the microglia staining. Another reason we considered, was if it could be something wrong with the primary Abs, and if the primary Ab bind non-specifically (45). This can be ruled out because the negative control was never incubated with primary Abs. The tissue was fixated with 4% PFA solution, and the solution itself could produce a fluorescent signal at green wavelengths. When using a fluorophore with excitation at another wavelength, this problem can be fixed (45). The microglia fluorophore (Alexa Fluor 594) has optimal excitation wavelength at 594 nm, so when using this, background staining was not a problem (45).

4.3 Strengths and limitations

One of the strengths in this project is the use of rat models. The advantage of using rats is that rat brains have several similarities to the human brain when it comes to structure and functions. The use of these models is therefore a good alternative for studying human diseases and pathological changes when such experiments on humans are not feasible. Any kind of investigation of AD pathology is only possible post mortem, which is very limiting in humans. It is also worth mentioning that if humans had been used in these kinds of studies, it would have been more difficult to control the different aspects of the experiment, such as monitoring the amount and the intensity of PA of the exercised donors, and that the sedentary group had been inactive. Potentially, the quality of the donated plasma could have varied, thus it would have been difficult to assess the effect of the treatment. By using rats, it is easier with a closer follow-up and to control the whole process.

Another strength is the use of confocal microscopy compared to regular fluorescence microscopy. This allows three-dimensional imaging (z-stack in several planes), in addition to providing great images with high resolution and contrast in thick tissue. The use of an indirect immunofluorescence technique in this project, is another strength, compared to a direct method. The indirect method requires more time, but due to the ability of several fluorophore-labeled secondary Abs to bind to a single Ag-bounded primary Ab, this method will give a stronger detectable signal, which increases the method's sensitivity.

Immunofluorescence is a specific technique due to the use of specific Abs that target specific Ags of interest, in this case A β and microglial cells. A fluorescence signal should therefore indicate that what is of interest has been detected. However, problems such as autofluorescence as in this case, can interfere with the outcome.

A limitation in this project that should be mentioned is that immunofluorescence has been performed on relatively few brain sections, a total of 10 individuals divided into the three different groups. The results are therefore based on a small number of samples, which is not necessarily representative. To be able to conclude whether exercised plasma treatment has an effect, a larger number of individuals and sections should have been studied. Plasma from exercised donors of the same age as the recipients could also be used to exclude the potential effect of age-related factors on the results.

5.0 Conclusion

To conclude, we found that ExPlas rats had more similar microglia morphology to the wild-type rats compared to the AD rats. This indicates that young, exercised plasma treatment on AD rats may prevent microglial activation, and then strengthen the hypothesis that exercised plasma has a beneficial effect on microglial activity. Whether this could be due to less A β in ExPlas rat, could not be concluded by these results but is something that could be further investigated. In this project, the results for A β could not be evaluated, because of presumed high autofluorescence, most likely induced by mitochondria and/or lysosomes. The hypothesis that ExPlas rats have less A β accumulation than AD rats and more similarities to wild-type rats could not be answered. In addition to this, it was not feasible to consider the connection between A β and microglial cells.

In order for the study to be more representative, and to be able to conclude that exercised plasma has an effect on microglial cells and A β accumulation, further studies should use more samples, and include samples where the donors are of the same age as the recipients. Further investigations could also use tissue that had been stored for shorter time, or change the fluorophore, to achieve better A β results.

Importantly and despite these drawbacks, current project results show significant differences between the length of the branches and the increased endpoints in ExPlas rats compared to AD rats. This is promising results, and further studies on this field, could lead to important findings for Alzheimer's disease treatment.

6.0 References

1. Tari AR, Norevik CS, Scrimgeour NR, Kbro-Flatmoen A, Storm-Mathisen J, Bergersen LH, et al. Are the neuroprotective effects of exercise training systemically mediated? *Progress in Cardiovascular Diseases*. 2019 Mar 1;62(2):94–101.
2. 2021 Alzheimer's disease facts and figures. *Alzheimer's & Dementia*. 2021;17(3):327–406.
3. Silva MVF, Loures C de MG, Alves LCV, de Souza LC, Borges KBG, Carvalho M das G. Alzheimer's disease: risk factors and potentially protective measures. *J Biomed Sci*. 2019 May 9;26(1):33.
4. Villeda SA, Plambeck KE, Middeldorp J, Castellano JM, Mosher KI, Luo J, et al. Young blood reverses age-related impairments in cognitive function and synaptic plasticity in mice. *Nat Med*. 2014 Jun;20(6):659–63.
5. Dementia WHO [Internet]. [cited 2022 Mar 22]. Available from: <https://www.who.int/news-room/fact-sheets/detail/dementia>
6. ExPlas-studien - CERG - NTNU [Internet]. [cited 2022 Apr 6]. Available from: <https://www.ntnu.no/cerg/explas>
7. Rodríguez JJ, Verkhatsky A. Neurogenesis in Alzheimer's disease. *Journal of Anatomy*. 2011;219(1):78–89.
8. 2022 Alzheimer's disease facts and figures. *Alzheimer's & Dementia* [Internet]. 2022; Available from: <https://dx.doi.org/10.1002/alz.12638>
9. Tiwari S, Atluri V, Kaushik A, Yndart A, Nair M. Alzheimer's disease: pathogenesis, diagnostics, and therapeutics. *International Journal of Nanomedicine*. 2019;Volume 14:5541–54.
10. Leng F, Edison P. Neuroinflammation and microglial activation in Alzheimer disease: where do we go from here? *Nat Rev Neurol*. 2021 Mar;17(3):157–72.
11. Anand KS, Dhikav V. Hippocampus in health and disease: An overview. *Ann Indian Acad Neurol*. 2012;15(4):239–46.
12. Paul SM, Reddy K. Young blood rejuvenates old brains. *Nat Med*. 2014 Jun;20(6):582–3.
13. Leon WC, Canneva F, Partridge V, Allard S, Ferretti MT, DeWilde A, et al. A novel transgenic rat model with a full Alzheimer's-like amyloid pathology displays pre-plaque intracellular amyloid-beta-associated cognitive impairment. *J Alzheimers Dis*. 2010;20(1):113–26.
14. Carlesimo GA, Piras F, Orfei MD, Iorio M, Caltagirone C, Spalletta G. Atrophy of presubiculum and subiculum is the earliest hippocampal anatomical marker of Alzheimer's disease. *Alzheimers Dement (Amst)*. 2015 Mar 29;1(1):24–32.
15. Swanson LW. Brain maps 4.0—Structure of the rat brain: An open access atlas with global nervous system nomenclature ontology and flatmaps. *J Comp Neurol*. 2018 Apr 15;526(6):935–43.

16. Ali S, Liu X, Queen NJ, Patel RS, Wilkins RK, Mo X, et al. Long-term environmental enrichment affects microglial morphology in middle age mice. *Aging (Albany NY)*. 2019 Apr 29;11(8):2388–402.
17. Hansen DV, Hanson JE, Sheng M. Microglia in Alzheimer’s disease. *Journal of Cell Biology*. 2018;217(2):459–72.
18. Huuha AM, Norevik CS, Moreira JBN, Kobro-Flatmoen A, Scrimgeour N, Kivipelto M, et al. Can exercise training teach us how to treat Alzheimer’s disease? *Ageing Research Reviews*. 2022 Mar 1;75:101559.
19. Ross R, Blair SN, Arena R, Church TS, Després JP, Franklin BA, et al. Importance of Assessing Cardiorespiratory Fitness in Clinical Practice: A Case for Fitness as a Clinical Vital Sign: A Scientific Statement From the American Heart Association. *Circulation*. 2016 Dec 13;134(24):e653–99.
20. Horowitz AM, Fan X, Bieri G, Smith LK, Sanchez-Diaz CI, Schroer AB, et al. Blood factors transfer beneficial effects of exercise on neurogenesis and cognition to the aged brain. *Science*. 2020 Jul 10;369(6500):167–73.
21. Kim TW, Park SS, Park JY, Park HS. Infusion of Plasma from Exercised Mice Ameliorates Cognitive Dysfunction by Increasing Hippocampal Neuroplasticity and Mitochondrial Functions in 3xTg-AD Mice. *Int J Mol Sci*. 2020 May 6;21(9):E3291.
22. De Miguel Z, Khoury N, Betley MJ, Lehallier B, Willoughby D, Olsson N, et al. Exercise plasma boosts memory and dampens brain inflammation via clusterin. *Nature*. 2021 Dec;600(7889):494–9.
23. Poon CH, Wang Y, Fung ML, Zhang C, Lim LW. Rodent Models of Amyloid-Beta Feature of Alzheimer’s Disease: Development and Potential Treatment Implications. *Aging Dis*. 2020 Oct 1;11(5):1235–59.
24. Ellenbroek B, Youn J. Rodent models in neuroscience research: is it a rat race? *Dis Model Mech*. 2016 Oct 1;9(10):1079–87.
25. Iulita MF, Allard S, Richter L, Munter LM, Ducatenzeiler A, Weise C, et al. Intracellular A β pathology and early cognitive impairments in a transgenic rat overexpressing human amyloid precursor protein: a multidimensional study. *Acta Neuropathol Commun*. 2014 Jun 5;2:61.
26. Magaki S, Hojat SA, Wei B, So A, Yong WH. An Introduction to the Performance of Immunohistochemistry. *Methods Mol Biol*. 2019;1897:289–98.
27. Rifai N, Horváth AR, Wittwer CT. *Tietz fundamentals of clinical chemistry and molecular diagnostics*. Eighth edition. St. Louis, Missouri: Elsevier; 2019. s. 237-238
28. Odell ID, Cook D. Immunofluorescence Techniques. *Journal of Investigative Dermatology*. 2013 Jan;133(1):1–4.
29. Nelson PN, Reynolds GM, Waldron EE, Ward E, Giannopoulos K, Murray PG. Demystified ...: Monoclonal antibodies. *Molecular Pathology*. 2000 Jun 1;53(3):111–7.
30. Roald B. immunhistokjemi. In: *Store medisinske leksikon* [Internet]. 2020 [cited 2022 Apr 6]. Available from: <http://sml.snl.no/immunhistokjemi>

31. Vikse J. antistoffer. In: Store medisinske leksikon [Internet]. 2022 [cited 2022 Apr 29]. Available from: <http://sml.snl.no/antistoffer>
32. IHC antigen retrieval protocol | Abcam [Internet]. [cited 2022 May 5]. Available from: <https://www.abcam.com/protocols/ihc-antigen-retrieval-protocol>
33. Jensen EC. Types of Imaging, Part 2: An Overview of Fluorescence Microscopy. *The Anatomical Record*. 2012;295(10):1621–7.
34. Sanderson MJ, Smith I, Parker I, Bootman MD. *Fluorescence Microscopy*. Cold Spring Harb Protoc. 2014 Jan 10;2014(10):pdb.top071795.
35. Emerging LED Technologies for Fluorescence Microscopy | Excelitas [Internet]. [cited 2022 May 10]. Available from: <https://www.excelitas.com/editorials/emerging-led-technologies-fluorescence-microscopy>
36. Autofluorescence - an overview | ScienceDirect Topics [Internet]. [cited 2022 May 2]. Available from: <https://www.sciencedirect.com/topics/medicine-and-dentistry/autofluorescence>
37. Monici M. Cell and tissue autofluorescence research and diagnostic applications. *Biotechnol Annu Rev*. 2005;11:227–56.
38. Wang YL, Grooms NWF, Civale SC, Chung SH. Confocal imaging capacity on a widefield microscope using a spatial light modulator. *PLoS One*. 2021 Feb 16;16(2):e0244034.
39. Elliott AD. *Confocal Microscopy: Principles and Modern Practices*. *Curr Protoc Cytom*. 2020 Mar;92(1):e68.
40. Kilpatrick CW. Noncryogenic preservation of mammalian tissues for DNA extraction: an assessment of storage methods. *Biochem Genet*. 2002 Feb;40(1–2):53–62.
41. Goat Anti Mouse (IgG) secondary antibody cross-adsorbed Alexa Fluor® 488 [Internet]. [cited 2022 May 3]. Available from: <https://www.abcam.com/goat-mouse-igg-hl-alex-fluor-488-preadsorbed-ab150117.html?productWallTab=ShowAll>
42. Young K, Morrison H. Quantifying Microglia Morphology from Photomicrographs of Immunohistochemistry Prepared Tissue Using ImageJ. *J Vis Exp*. 2018 Jun 5;(136):57648.
43. Mosher KI, Wyss-Coray T. Microglial dysfunction in brain aging and Alzheimer’s disease. *Biochemical Pharmacology*. 2014 Apr 15;88(4):594–604.
44. Fixation using Paraformaldehyde [Internet]. 2019 [cited 2022 May 15]. Available from: <https://qbi.uq.edu.au/fixation-using-paraformaldehyde>
45. IHC Troubleshooting | Abcam [Internet]. [cited 2022 May 15]. Available from: <https://www.abcam.com/help/troubleshooting-and-using-controls-in-ihc-and-icc#high-background>

7.0 Appendix

Appendix I: Overview of the preclinical ExPlas study

Wild-type (non-transgenic) Wistar donor rats at the age of two months were randomly divided into two groups; one group that exercised according to a 6-week long training protocol, and the other group consisting of sedentary rats that were left in their cage and kept away from training for 6 weeks. During the exercise period, the rats were exercised for 5 times per week. The exercise sessions in the protocol consisted of high-intensity intervals on treadmills. Each session started with 10 minutes of warm-up followed by ten 4-minute intervals separated by periods with active resting.

Before and after the exercise period, the Wistar donor rats underwent cardiorespiratory fitness testing, which showed that they had improved their maximal oxygen consumption (VO₂ max) before exercised plasma donation.

Plasma collection

After 6 weeks, blood from both donor groups were collected for plasma donation. The exercised rats' and the sedentary rats' entire blood volume was collected via cardiac puncture, during deep anesthesia, before the rats were subsequently sacrificed. The collected blood was centrifuged before plasma was distributed in tubes and stored at -80 °C for further use and injections.

Injection treatment

During a period of 6 weeks, the AD rats (McGill-R-Thy1-APP model) received plasma injection treatment donated from the Wistar donor rats starting at the age of 5 months. The AD rats were divided into three groups, where each group received one of three possible treatments: exercised plasma (ExPlas), sedentary plasma (SedPlas), or saline (negative control group). The treatment consisted of 14 intravenous injections which were injected under anesthesia into the rats' tail vein, each injection with a volume of 2 mL per kg body weight.

Formalin-fixation and brain tissue sectioning

The rats were transcardially perfused with 4% paraformaldehyde solution for tissue fixation. The brains were collected and left in 4% paraformaldehyde solution for 24 hours before they were transferred in new tubes with dimethyl sulfoxide solution (DMSO). The brains were coronally sectioned to 40 μm sections using a freezing microtome (Microm HM430, Thermo Fisher Scientific).

Appendix II: Overview of the rat models

Table 2. Rat-ID and their condition included in the four different days of staining.

	Rat model	Rat model	Rat model	Positive control	Negative control
First staining	ID: 23748 6 months AD rat	ID: 23735 6 months Wild-type rat	-	ID: B336F 12 months AD rat	ID: 23748 12 months AD rat
Second staining	ID: 23764 6 months AD rat	ID: 23749 6 months Wild-type rat	-	ID: B336F 12 months AD rat	ID: B336F 12 months AD rat
Third staining	ID: 23761 6 months AD rat	ID: 23750 6 months Wild-type rat	ID: #63 6 months ExPlas rat	ID: B336F 12 months AD rat	ID: B336F 12 months AD rat
Fourth staining	ID: #50 6 months ExPlas rat	ID: #54 6 months ExPlas rat	ID: #61 6 months ExPlas rat	ID: B43E4 12 months AD rat	ID: B43E4 12 months AD rat

An additional staining with the preadsorbed secondary antibody was performed as a fifth staining and included one section from each of these rats.

Appendix III: Staining protocol for detecting amyloid-beta and microglial cells

Day 1

1. Use petridish with DMSO when selecting the sections.

Demasking

2. Preheat both waterbath and Sodium Citrate buffer (10mM sodium citrate, 0.05% Tween, pH=6,0) to +80 °C.
3. Transfer free-floating brain sections into eppendorf tubes or brain cups containing preheated Sodium Citrate buffer and keep in the preheated water bath (+80 °C).
4. Maintain this temperature for **45** min.
5. Take out of water bath and retrain sections in the solution until room temperature is reached.
6. Rinse sections 3 x 10 min in TBS.

Blocking

7. Incubate in 10% goat serum in TBS-Tx for 1 hour.

Primary antibodies

8. Draw off excess solution (do not wash). Incubate sections with primary antibodies in TBS-Tx: **Mouse monoclonal antibody to Amyloid beta 1-42 (1:500) and Rabbit monoclonal to Iba1 (1:2000) overnight at +4°C.**
 - Remember negative control with only TBS-Tx.

Day 2

9. Rinse sections 3 x 10 min in TBS-Tx.
10. Incubate sections with secondary antibodies in TBS for 1 hour, **Goat Anti-Mouse IgG H&L Alexa Fluor 488 (1:667) and Goat anti-rabbit IgG H&L Alexa Fluor 594 (1:500)**. Cover with aluminium foil.
11. Rinse 2x5 min in TBS. Incubate with DAPI (1:2000) for 2 min. Rinse 5 min in TBS.
 - Keep covered with aluminium foil.
 - For later mounting, keep in TBS in the fridge, covered with foil.
12. Mount sections and coverslip on glass slides.
 - Mount while section is floated in TBS - let dry for at least 30 min.
 - Add a few small drops of vectashield and place coverslip without adding too much pressure. Seal the coverslip using nailpolish. Let dry in the dark.
13. Mounted sections can be stored (in the dark) for up to 6 months in a refrigerator at +4°C.

Appendix IV: Solutions preparing for the immunostaining protocol

- **Phosphate buffer (PB) 0,4 M.** Prepare solutions A and B. A (acid): Dissolve 13,8 g Sodium dihydrogen phosphate ($\text{NaH}_2\text{PO}_4 \cdot \text{H}_2\text{O}$) in 250 mL H_2O . B (base): Dissolve 17,8 g Sodium hydrogen phosphate dihydrate ($\text{Na}_2\text{H}_2\text{PO}_4 \cdot 2\text{H}_2\text{O}$) in 250 mL H_2O . Add solution A to solution B until the pH is 7.4. Store in the dark in room temperature for up to one month.
- **Dimethyl sulfoxide (DMSO):** To make 100 mL, mix 31.25 mL of 0.4M phosphate buffer, 46.75 mL H_2O , 20 mL glycerine, and 2 mL DMSO.
- **Sodium citrate buffer** (10mM Sodium Citrate, 0.05% Tween-20, pH 6.0). Tri sodium citrate (dihydrate) 2.94 g + 1 L H_2O . Mix to dissolve. Adjust pH to 6.0 with 1 M HCl. Add 0.5 mL Tween-20 and mix well.
- **Tris-buffered saline (TBS) pH 8.0.** For 1500 mL: dissolve 9.09 g Tris + 13.44 g NaCl in 1500 mL H_2O . Adjust pH to 8.0 with HCl (2,0 M). Store in refrigerator for up to one week.
- **TBS-Tx (0.5 %) pH 8.0.** In a ventilated hood, add 2,5 mL of Triton X-100 to 500 mL TBS and mix well. Store in refrigerator for up to one week.
- **HCl 2 M.** For 50 mL: Add 8.4 mL of 37 % HCl to 41.6 mL H_2O . Do not make the mistake of adding water to concentrated HCl. Store in room temperature in a well-ventilated place for an extended period of time.
- **Primary antibody (Ab42):** Mouse monoclonal to Beta Amyloid 1-42 (12F4). Biolegend, Cat# 805501. RRID:[AB_10732141](#).
- **Primary antibody (Iba1, *ionized calcium binding adaptor molecule 1*):** Rabbit monoclonal [EPR16588] to Iba1. Abcam, Cat# ab178846. RRID:[AB_2636859](#).
- **Secondary Antibody (for Ab42):** Goat Anti-Mouse IgG H&L (Alexa Fluor 488) antibody. Abcam, Cat# ab150113. RRID:[AB_2576208](#). 2 mg/mL. Store at 2 - 8°C. LOT #GR3419505-1.
- **Secondary Antibody (for Iba1):** Goat Anti-Rabbit IgG H&L (Alexa Fluor 594) antibody. Abcam, Cat# ab150080. RRID:[AB_2650602](#). 2 mg/mL. Store at 2 - 8 °C. LOT #GR3401492.
- **Goat serum:** Normal goat serum, Invitrogen. Store at -20°C. Ref: 10000C. LOT # 1115869A.
- **VECTASHIELD**, antifade mounting medium. store at 2 - 8 °C. LOT # ZF0612. Ref: 3 H-1000.

